On the Homoclinic Tangles of Henri Poincaré

Qiudong Wang

1. Introduction

It is well acknowledged that Poincaré's discovery of homoclinic tangles marked the beginning of the modern chaos theory ([31], [32]). Poincaré studied differential equations in the form of

$$\frac{dx}{dt} = f(x) + \varepsilon g(x,t) \tag{1.1}$$

where $x \in \mathbb{R}^n$ is the phase variable, $g(x,t)$ is a time-periodic forcing function, and ε is a small parameter. He observed that, in the vicinity of homoclinic solutions of a saddle fixed point x_0 of the unperturbed equation, time-periodic perturbations $\varepsilon g(x,t)$ induce complicated dynamic structures, which he named as *homoclinic tangles*.

In this paper, we introduce to the reader a theory on the homoclinic tangles of equation (1.1) ([44], [45]). The objective of this theory is to understand the dynamics of the invariant sets of solutions of equation (1.1) in the vicinity of the unperturbed homoclinic solutions. Since equation (1.1) is with a small parameter ε, this objective is divided into two: the first is to describe the dynamics of a homoclinic tangle for a fixed value of ε and the second is to tell in what way the tangles of different ε fits together.

We assume (i) $n = 2$ so $x \in \mathbb{R}^2$ and (ii) the saddle fixed point x_0 is *dissipative* in the sense that the negative eigenvalue of the Jacobian matrix $Df(x_0)$ is larger than the positive eigenvalue in magnitude. This theory ([44], [45]) asserts that Smale's horseshoe ([37]), SRB measure of Benedick-Carleson and Young ([34], [33], [8], [4], [6]), and Newhouse sinks ([27], [28]) are all participating elements of the homoclinic tangles of equation (1.1). This theory also asserts that, on parameter intervals of a fixed length of $\ln \varepsilon$, homoclinic tangles of different structures are arranged in a fixed pattern, and this pattern is repeated indefinitely as $\varepsilon \to 0$.

This exposition is divided into two parts. Sections 2-7 are the first part and Sections 8-10 are the second. In Sections 2 and 3 we recall the historic events that led to the discovery of homoclinic tangles and the prominent role homoclinic tangles of equation (1.1) played in this mathematical venture in history[1]. In Sections 4-7, we introduce the participating dynamic objects of the homoclinic tangles of equation (1.1). Section 4 is on the Smale Horseshoe. Section 5 is on the SRB measure for the Anosov diffeomorphism. Section 6 is on the theory of Hénon maps and the SRB measures of Benedick-Carleson and Young. Section 7 is on the Newhouse theory. Since the discoveries of the participating dynamic objects of homoclinic tangles of equation (1.1) were stretched over a long period of time and each of these discoveries has been an event of substantial influence on its own in the development of the modern theory of dynamical systems, this part also serves as a review on history. The scope of this review, however, is restricted to the dynamic objects related to the homoclinic tangles of equation (1.1). Our purpose is to introduce the theory of [44] and [45], and to put this theory in historic perspective for the reader.

[1]We note that Poincaré did not consider the dissipative case. In his study all that mattered were conservative equations.

In Sections 8 and 9, we present an overview on the dynamics of homoclinic tangles of equation (1.1), in which the dynamic objects introduced in the first part all come to participate. In Section 10, we present the result of a numerical simulation in conjunction with the theory presented in Sections 8 and 9.

This paper is not written exclusively for experts on the subject matter. It is also for people with a generic interest in modern chaos theory and its applications to ordinary differential equations. Sections 2-4 should be easy reading for a generic reader, but it is unseemly that a non-expert would have been exposed previously to all that is presented in Sections 5-7. Substantial efforts are put forth in the writing of these three sections to make the main conclusions of certain sophisticated dynamics theories accessible to non-experts.

2. King Oscar II's prize on the N-body problem

Our story started with a prized competition established by King Oscar II of Sweden and Norway in 1888 for solving the Newtonian N-body problem. Seeking to promote the newly launched *Acta Mathematica*, Gösta Mittag-Leffler, his Majesty's science adviser, prompted the King to set up this royal competition. The prize committee was comprised of Charles Hermite, Gösta Mittag-Leffler and Karl Weierstrass. Since the committee could not use a vague term such as *solving the N-body problem* to define the main objective of this competition, it first had to decide in precise terms a way in which the N-body problem could be deemed as a resolved mathematical problem. This task was delegated to Weierstrass.

At the time, there were very practical and rather urgent needs in Astronomy and in Navigation to use the solutions of the N-body problem to foretell the positions of celestial bodies. Nowadays, computer can do the job through numerical integration, but at the time people had to rely on power series solutions ([16], [50]). However, all power series solutions acquired for the N-body problem at the time converge only on finite time intervals, and the size of the convergence interval varies depending on the location of the solution. It is then quite natural that Weierstrass equated the mathematical task of solving the N-body problem to the task of finding a power series solutions that converges for all time. A rather carefully crafted formulation, formally introduced in the official announcement for the prized competition in *Acta Mathematica*, vol. 7, of 1885-1886, was as follows:

Given a system of arbitrarily many mass points that attract each other according to Newton's law, under the assumption that no two points ever collide, try to find a representation of the coordinates of each point as a series in a variable that is some known function of time and for all of whose values the series converges uniformly.

The proposed power series solutions were constructed by Karl Sundman twenty six years later for the 3-body problem ([41], [35])), and by myself at a much later time for all N ([43]). In both cases, however, the power series constructed converge so slowly that they were practically useless. My construction, in particular, is *tricky* but surprisingly *simple*. A question with a tricky, simple, and useless answer is not the kind the prize committee ought to have asked. This, therefore, was their first mathematical mistake.

Henri Poincaré started working on the proposed problem. In a letter addressed to Mittag-Leffler, Poincaré claimed to have proven a stability result for the restricted three-body problem. He wrote ([14], page 44)

In this particular case, I have found a rigorous proof of stability and a method of placing precise limits on the elements of the third body... I now hope that I will be able to attack the general case and ... if not completely resolve the problem (of this I have little hope), then at least found sufficiently complete results to send into the competition.

Soon after, Poincaré submitted his paper, and was awarded the prize. His paper was dually refereed by Mittag-Leffler and Weierstrass, and the latter asserted in his report to the former that ([14], page 44)

I have no difficulty in declaring that the memoir in question deserves the prize. You may tell your Sovereign that this work can not, in truth, be considered as supplying a complete solution to the question we proposed, but it is nevertheless of such importance that its publication will open a new era in the history of celestial mechanics. His Majesty's goal in opening the contest can therefore be considered attained.

It was, however, soon realized that Poincaré's prize winning paper contained a fatal mathematical error, and the stability result he claimed to Mittag-Leffler was wrong. It appeared that Poincaré himself spotted the fatal error when answering certain questions raised by Edvard Phragman, who was copy editing Poincaré's paper to be published by Acta Mathematica.

The mistake made by the committee to award a grand prize to a paper with a fatal mathematical error was an unpleasant reality with which Mittag-Leffler had to reckon. When the mistake was uncovered, Poincaré's original submission was already in print. Mittag-Leffler decided to make a recall, and ordered all copies with Poincaré's original paper to be physically destroyed. Poincaré paid twice as much as the prize money he received to cover the cost of this recall. Mittag-Leffler was in a real difficult situation. He needed to maintain a high scientific and ethic standard and, at the same time, to control a potential fallout that was at the very least a great embarrassment. After all, there were others who had put forth great effort in participating in this competition and were arguing that their work was more deserving to win the prize.

In trying to reckon with the *mathematical* consequences of his mistake, Poincaré discovered homoclinic tangles therefore gave birth to the chaos theory, a mathematical theory of great influence in later times. Poincaré's paper, published by *Acta Mathematica* after the recall ([31]), is a true masterpiece and is that history has proven to equal all that was asserted in Weierstrass's report.

3. Discovery of Homoclinic tangles

Mittag-Leffler's order to destroy all recalled copies of Poinacré's original submission was not thoroughly carried out. At least one copy was uncovered one hundred years later by Richard McGehee, whose research was primarily on the three-body problem.[2]

To understand the error in Poincaré's paper and the mathematical discovery that followed, we start with the geometric method Poincaré introduced in the study of ordinary differential equations ([30]). Let $x = (x_1, \cdots, x_n)$ be an n-vector and t be the time. Let

$$\frac{dx}{dt} = f(x) \tag{3.1}$$

be a set of ordinary differential equations for x. Before the time of Poincaré, mathematicians had tried to *solve* equation (3.1) by deriving *explicit* formula of solutions of x in t. Since solutions in closed form are in general not attainable, power series were used as a substitute.

Poincaré's geometric point of view, which was truly revolutionary at the time, is to treat equation (3.1) as a *geometric*, not an *analytic*, problem. He viewed x as a point in $\mathbb{R}^n$, which

[2]McGehee introduced a new set of variables to study the solutions of the N-body problem near triple collision ([22]). His new variables were used to construct solutions of non-collision singularity for the N-body problem ([51]). My construction of the aforementioned power series solution was also based on a modified version of McGehee's coordinates.

he called the *phase space*, and solutions of equation (3.1) as a collection of non-intersecting curves in phase space. He pointed out that the correct way to study equation (3.1) is not to chase after an impossible solution formula, but to ask (a) what kind of solution curves are allowed by equation (3.1), and (b) in what way all solution curves fit together.

The equation for the restricted three-body problem, on which Poincaré was toiling for the King's prize, was not exactly like equation (3.1). It is in the form of

$$\frac{dx}{dt} = f(x) + \varepsilon g(x,t) \tag{3.2}$$

where ε is a small parameter and $g(x,t)$ is a function that is periodic in t, say, of period T. One good thing about the restricted 3-body problem, which was the subject of Poincaré's investigation, is that the equation for $\varepsilon = 0$ is completely solvable, so he knew everything about the solution curves and the way they fit together. In particular, he knew that there is an equilibrium solution, to which a family of solutions asymptotically approach in both the backward and the forward time. Poincaré called these solutions *homoclinic*. Homoclinic solutions form a nice invariant surface in phase space when $\varepsilon = 0$. Now the question is what happens to this nice invariant surface when ε is not zero? Here Poincaré mistakenly argued that this invariant surface remained intact. This is, unfortunately, not at all the case.

Let $x(t, x_0, \varepsilon)$ be the solution of (3.2) satisfying $x(0, x_0, \varepsilon) = x_0$. Poincaré introduce a map $F_\varepsilon : x_0 \to x(T, x_0, \varepsilon)$ induced by the solutions of equation (3.2) and pointed out that to study the solutions of equation (3.2) is the same as to study the iterations of F_ε, which he named as the *time-T map*. See Figure 1.

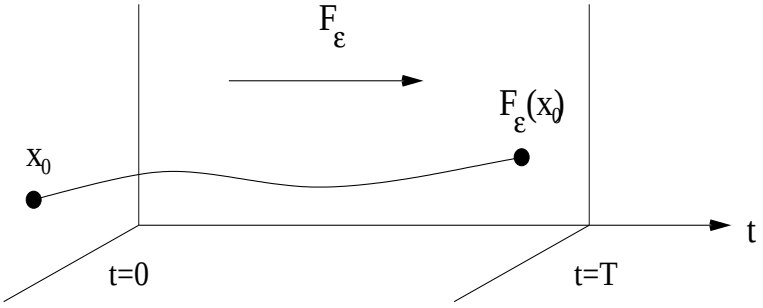

Figure 1. The time-T map

Now assume $n = 2$ so $x \in \mathbb{R}^2$. For equation (3.2), F_ε is a one parameter family of maps and ε is the parameter. Let ℓ_0 be the trajectory of a homoclinic solution of the unperturbed equation ($\varepsilon = 0$) in phase space. We have $F_0(\ell_0) = \ell_0$. This is to say that ℓ_0 is an *invariant loop* of F_0, the time-T map for the unperturbed equation. See Figure 2(a). Small perturbation, unfortunately, would break this loop into two intersecting curves, one of which we denote as ℓ^s_ε and name as the stable manifold, and the other we denote as ℓ^u_ε and name as the unstable manifold. See Figure 2(b).

Take a small piece of the unstable manifold around the point of intersection, and map it forward in time. Poincaré reasoned that the images of this piece under the iteration of F_ε would eventually follow the unstable manifold to come back to intersect the stable manifold again. See Figure 3(a). Likewise, a small piece of stable manifold around the point of intersection would be mapped backward, eventually following the stable manifold to induce new intersections. Consequently, the stable and unstable manifold would form a web, the structure of which appeared to be incomprehensibly complicated. See Figure 3(b). For

solutions in this complicated mesh, which he called a *homoclinic tangle*, dynamical stability appeared unlikely.

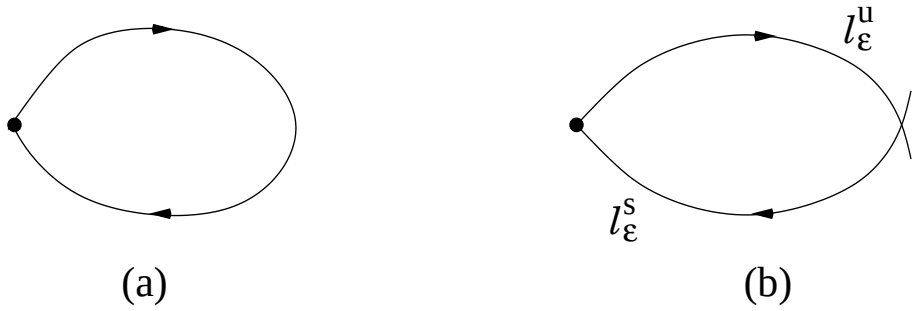

Figure 2. Non-tangential intersection of stable and unstable manifold

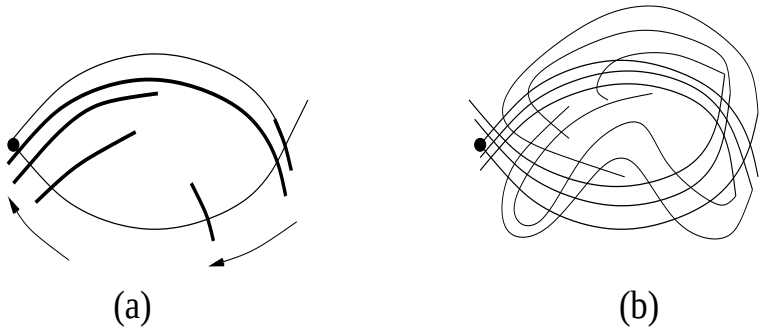

Figure 3. Formation of homoclinic tangle

From the time of Henri Poincaré to the early 1960's, many people, including Birkhoff ([7]), Cartwright and Littlewood ([9]), Levinson ([17]), Sitnikov ([40]) and Alekseev ([1]), had studied homoclinic tangles in differential equations. Some had also come to the conclusion that periodic solutions accumulate in homoclinic tangles.

4. Smale's Horseshoe

The next breakthrough was brought along by Stephen Smale in early 1960s in correcting one wrong conjecture of his own. Smale came to world renown by his work on the Poincaré conjecture[3] in algebraic topology ([36]). His study was based on the Morse theory, which is a study on gradient-like equations defined on compact manifold ([24]). He then ventured into the study of other differential equations and conjectured that accumulations of periodic orbits are vulnerable to small perturbations. At the time, Smale was not aware of the work of Poincaré and others on homoclinic tangles. After Levinson introduced these studies to him, and pointed out that these results are in direct contradiction to his conjecture, Smale realized that there is a rather *simple* geometric structure embedded in *all* homoclinic tangle, and that this structure produces accumulations of periodic solutions and other complicated dynamical behavior ([37]).

[3]Poincaré's invention of algebraic topology is not entirely unrelated to his study of the N-body problem. See [21].

The geometric structure Smale introduced is as follows. Let us start with a 2D square. We first compress it in the vertical direction and stretch it in the horizontal direction to make a thin and long strip. We then fold the strip and put it back on the original square. See Figure 4(a). This defines a map, which Smale called a *horseshoe map*.

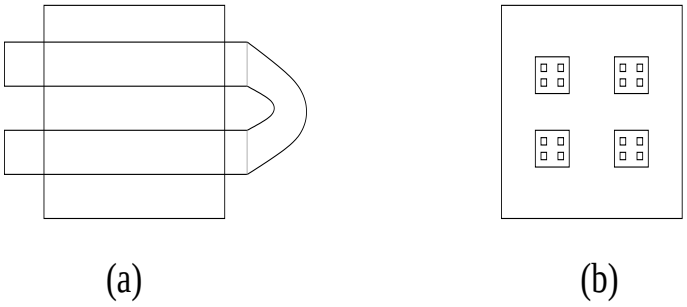

Figure 4. Smale's horseshoe

Under the horseshoe map, part of the square is mapped out and part is mapped back into the square. Smale observed that there is a subset that would stay inside of the square forever under the forward and the backward iterations of the horseshoe map, and this set has a complicated but thoroughly understandable structure. A conceptual way to comprehend the structure of this invariant set is to forever replace every square by four smaller squares inside, starting with the original square. See Figure 4(b). It is not hard to show that this invariant subset contains infinitely many periodic orbits of saddle type.

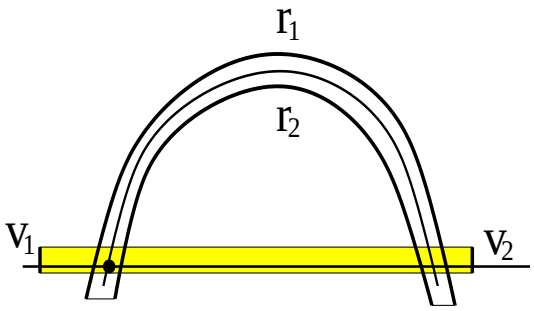

Figure 5. Horseshoe embedded inside of a homoclinic tangle

Smale illustrated that every homoclinic tangle contains a horseshoe. This is shown in Figure 5. Starting with a horizontal strip containing a segment of the stable curve, as drawn in Figure 5. Denote the vertical boundaries of this strip as v_1 and v_2 respectively. Iterating by using the time-T map, the image of v_1 would eventually become the arc labeled as r_1, and v_2 as r_2, in Figure 5. To turn this figure around 90 degrees, we would see Figure 4(a).

The elegance and the simplicity of Smale's construction made a very complicated mathematical situation accessible to even non-mathematicians. Together, with the later discoveries of similar elegance and simplicity, such as the *Lorenz butterfly* ([20]), Li-York's *period three implies chaos* ([18]), and Feigenbaum's *periodic doubling diagram* ([12]), it generated great enthusiasm for the chaos theory in the general scientific community in 1970s and 1980s.

5. Anosov Diffeomorphism and SRB Measure

To define and to study homoclinic tangles, we do not have to start with a differential equation. To induce a homoclinic tangle following Poincaré's observation, all it takes is to have a map with a transversal intersection of the stable and unstable manifold of a saddle fixed point (See Figure 2(b)). Maps with homoclinic tangle are easy to come up with and iterating a map is much easier than solving a differential equation. Therefore, it was almost like a liberation when the attention was gradually shifted from equations to maps. Questions of independent mathematical interest arose and dynamical systems as a research subject exploded. In this history of fascinating progresses, two maps have commanded tremendous attention. They are the *Anosov diffeomorphism* ([3]) and the *Henon maps* ([15]).

Anosov diffeomorphism is a map for which the *entire phase space* is one homoclinic tangle. The phase space is the 2D torus $\mathbb{T}^2 = \mathbb{R}^2/\mathbb{Z}^2$, and this map is induced on $\mathbb{T}^2$ by the linear map

$$x_1 = 2x + y, \qquad y_1 = x + y. \tag{5.1}$$

Thanks to the simplicity of (5.1), the dynamic structure of this homoclinic tangle is thoroughly comprehensible. It is nonetheless complicated: (i) periodic orbits are dense on $\mathbb{T}^2$ and they are all saddles, (ii) the stable and unstable manifold of periodic orbits wrap around the 2D torus, each as a dense curve, and (iii) stable and unstable curves intersect transversally and the points of intersection are also dense in $\mathbb{T}^2$.

All periodic orbits and their stable and unstable manifold, however, are collectively a zero measure set on the 2D torus. Deleting this zero measure set, what remains is still a set of full measure. In this remainder set of full Lebesgue measure, individual orbits behave rather erratically in the sense that they all jump around without any allotted sense of destination. Such disorderly behavior was then characterized and commonly referred to as a *chaos*.

It has turned out, however, that in this chaos there exists a *law of statistics* that governs the asymptotic behavior for all: the asymptotic distributions of points of individual orbit in phase space are *the same* for almost all orbits. This governing law of statistics has been commonly referred to as an SRB measure. The theory of SRB measures was independently developed by Sinai ([34]), Ruelle ([33]) and Bowen ([8]) for *uniformly hyperbolic systems*[4], of which Anosov diffeomorphism is a distinguished example.

However, chaos and SRB measure presented in Anosov Diffeomorphism are induced exclusively by the non-trivial topology of the 2D torus. The underlining map (5.1) for this homoclinic tangle is linear. Chaos in homoclinic tangles of equation (3.2), on the other hand, are induced into existence by *shearing* in phase space enacted through nonlinear terms in the defining equation. Chaos in Anosov diffeormorphism are intrinsically different from *shearing induced chaos* ([49], [19]). Consequently, the conclusions of the study of Anosov diffeomorphism and its extension on *uniformly hyperbolic systems* can not be directly applied to homolinic tangle of equation (3.2). With this in mind we now move on to the study of Hénon maps.

6. Theory on Henon Maps

Henon maps are a two parameter family of 2D maps in the form of

$$x_1 = 1 - ax^2 + by, \qquad y_1 = bx \tag{6.1}$$

where a, b are parameters and $(x, y) \in \mathbb{R}^2$. This map was introduced by French astronomer Hénon in 1976 as a simple extension of the quadratic family $f(x) = 1 - ax^2$ to 2D. Hénon

[4]The precise statement for uniformly hyperbolic maps is slightly weaker: the attractive basin of an SRB measure is with a positive Lebesgue measure, not necessarily almost everywhere, in phase space.

numerically plotted the destinations of individual orbits for various values of parameters. For some parameters he plotted stable periodic orbits, but for others he plotted messy pictures as shown in Figure 6.

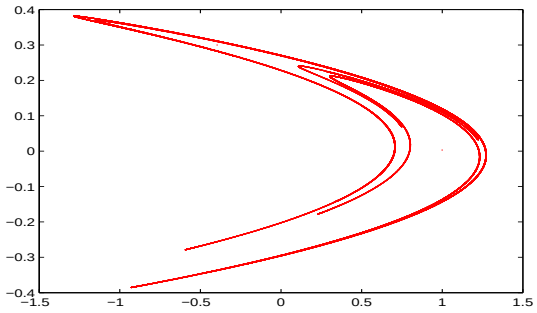

Figure 6. Strange attractors in Hénon maps

Asymptotically stable periodic orbits are natural destinations for other orbits. Their presence in numerical plots are rather expected because, when in existence, open sets of orbits are attracted to them.

It took awhile for a dynamics theory to emerge for the strange attractors plotted in Figure 6. With a *tour de force* analysis, Benedicks and Carleson ([4]) asserted that for the Hénon family there is a positive measure set of parameters, for which almost all orbits of the corresponding maps are unstable.[5] These maps admit *no stable periodic nor quasi-periodic orbits*. Here, we have a situation that is somewhat similar to *chaos* in Anosov diffeomorphism: since there exists nothing in phase space to offer an allotted destination, orbits would dance around, not knowing eventually where to go. For these *chaotic* maps, we would end up with the plot of Figure 6. We note that it is critically important for the set of parameters of chaotic Hénon maps to have a positive Lebesgue measure in parameter space; it implies that there is a positive probability they show up in numerical simulation.

The next step was to understand the dynamics of the object plotted in Figure 6. Equipped with Benedicks-Carleson's technical analysis of the Hénon maps, Benedicks and Young ([6]) proved that, for every chaotic Hénon map asserted in [4], there also exists a predestined asymptotic distribution for almost all orbits. This way, the theory of SRB measures was extended to cover chaotic Hénon maps. A complete dynamics profile for these maps was also provided later by Young and myself ([46]), with which we acclaimed a comprehensive understanding on the dynamics of the object plotted in Figure 6. It has turned out that, the dynamics of chaotic Hénon maps are quite different from that of the Anosov diffeomorphism: The dynamics of the latter is a sub-shift of finite type, all orbit of which can be coded by using a finite transition matrix. The former, though remains a sub-shift, is not of finite type therefore can not be coded by using transition matrix.

7. Homoclinic Tangency and Newhouse Theory

In previous sections, we have introduced two main dynamic objects: the Smale horseshoe and the SRB measure of Benedick-Carleson and Young. Smale's horseshoe is obviously a participating object in homoclinic tangles of equation (3.2), but to identify the SRB measure of Benedicks-Carleson and Young in the homoclinic tangles of equation (3.2) as a

[5]This statement is a little stronger than what Benedicks and Carleson were able to prove in [4], but they were close enough. The result as stated was first proved by Benedicks and Viana in [5].

participating object we would need to introduce yet another sophisticated dynamics theory. This is the Newhouse theory on homoclinic tangency ([27], [28]). With this theory we will also be able to extend our list of participating dynamic objects for the homoclinic tangles of equation (3.2) to include Newhouse sinks. In Sections 8 and 9, we will rely on the Newhouse theory to prove the existence of SRB measure of Benedick-Carleson and Young inside the homoclinic tangles of equation (3.2).

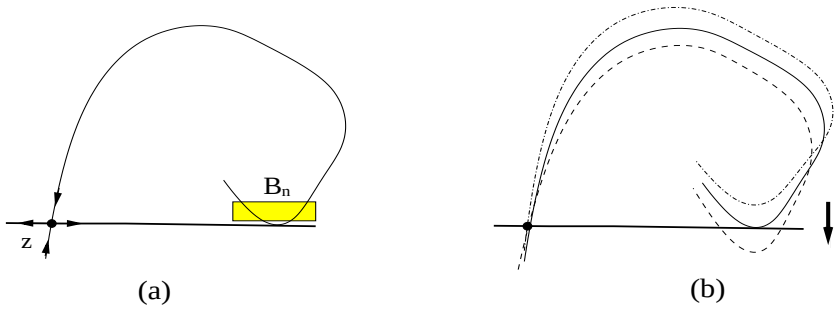

Figure 7. Transversal Homoclinic Tangecy

Newhouse studied a class of one parameter family of maps, in which he replaced the transversal intersection of the two curves in Figure 2(b) in Section 3 by a quadratic tangency. See Figure 7(a). He assumed that the saddle fixed point is *dissipative*, which is to say that the determinant of the Jacobian matrix at the saddle fixed point is with a magnitude < 1. He also assumed that as the parameter varies, the two curves at the point of tangency pass each other. See Figure 7(b).

By assuming that the fixed point is dissipative, Newhouse observed that there is a small rectangular box that would eventually be mapped back into itself (See Figure 7(a)). He re-scaled this box to size $\approx \mathcal{O}(1)$, and discovered that *the renormalized return maps are a perturbed Hénon family.*

Based on the Hénon-like formula obtained for the renormalized return maps, in particular on the fact that the renormalized return maps cover Hénon maps of parameters around small b and $a = 2$, Newhouse developed a rather sophisticated theory to concluded that (1) there are many other parameters, for which transversal homoclinic tangency exists, and (2) there are also infinitely many parameters for which the corresponding maps have asymptotically stable periodic orbits. Item (1) has been commonly characterized as the *persistency* of the Newhouse tangency, and item (2) as Newhouse's *infinite many sinks.*

Newhouse's theory appeared earlier than the theory of Benedicks and Carleson on Hénon maps. With this belated theory, a new dynamic scenario, the dynamics of chaotic Hénon maps, was added to the Newhouse theory. This addition was first worked out in detail by Mora and Viana ([25]). Combined with the work of Benedick and Young on the existence of SRB measures, it is concluded that, around any given value of parameter of Newhouse tangency, there are three infinite set of parameters, for which the corresponding maps respectively admit (a) Newhouse tangency, (b) asymptotically stable periodic orbits, or (c) SRB measure of Benedicks-Carleson and Young.

8. Infinitely Wrapped Horseshoe Map

We are finally ready to introduce the theory of [44] and [45] on the homoclinic tangles of time-periodic equations. We present the result of this theory in two steps. We first present an overview on the dynamics of a specific one parameter family of maps we name

as *infinitely wrapped horseshoe maps*. This is done in the current section. We then use the separatrix maps to convert the study of the homoclinic tangles of equation (3.2) to that of infinitely wrapped horseshoe maps. This is done in Section 9.

A one parameter family of infinitely wrapped horseshoe maps, which we denote as $\mathcal{T}_a$, is defined on the annulus $\mathcal{A} = \mathbb{S} \times [0,1]$ where $\mathbb{S} = \mathbb{R}/2\pi\mathbb{Z}$ is the unit circle. For $(\theta, y) \in \mathcal{A}$, we define $\mathcal{T}_a : (\theta, y) \to (\theta_1, y_1)$ by letting

$$\theta_1 = a + \theta - 10\ln(0.001y + \sin\theta), \qquad y_1 = 0.001\sqrt{0.001y + \sin\theta} \tag{8.1}$$

where $a \in (0, \infty)$. All maps in $\mathcal{T}_a$ are defined only on the part of $\mathcal{A}$ such that

$$0.001y + \sin\theta > 0.$$

Denote this defining domain as D. The boundaries of D cut $\mathcal{A}$ into two roughly rectangularly shaped regions. See Figure 8.

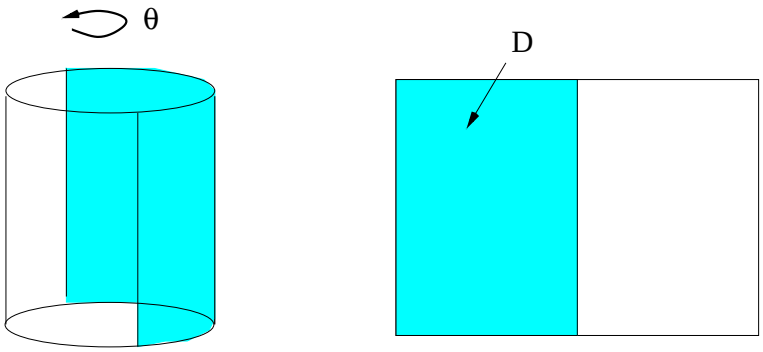

Figure 8. Domain of $\mathcal{T}_a$

The *objective* of our study is divided into *two* because $\mathcal{T}_a$ is a one parameter family. The first is on the dynamics of the invariant set of $\mathcal{T}_a$ for a fixed value of a, and the second is on the way the invariant sets for different values of a are fitted together in parameter space. On certain occasions a complete answer with mathematical rigor is attainable, but on other occasions, we can only extract answers that are partial in nature.

(a) The dynamics of individual invariant set The actions of a map $\mathcal{T}_a$ on D are as follows. First it compresses D in the y-direction, but stretches it in the θ-direction. Because of the logarithmic singularity, this image is stretched to infinite length at the vertical boundaries of D. This infinitely long strip is then folded at $\mathcal{T}_a(\theta, y)$ where $\theta \approx \tan^{-1} 100$ and placed back into $\mathcal{A}$, with the two infinitely long tails wrapping around $\mathcal{A}$ indefinitely. See Figure 9. In this figure the pre-image of the folded part is marked as V, and the folded image is marked as $\mathcal{T}_a(V)$. The dynamics of the invariant set of $\mathcal{T}_a$ are largely determined by *the location of the folded part of the image* $\mathcal{T}_a(V)$ *in* $\mathcal{A}$.

One obvious conclusion for $\mathcal{T}_a$ is that, for roughly half of the parameters $a \in [0, 2\pi]$, the folded part of the image $\mathcal{T}_a(V)$ is casted out of D. For these parameters the *entire invariant set of* $\mathcal{T}_a$ *is one horseshoe of infinite many branches*. See Figure 10. In this figure the horizontal strips are $D \cap \mathcal{T}_a(D)$, and the vertical strips are $\mathcal{T}^{-1}(D \cap \mathcal{T}_a(D))$. The structure of a horseshoe of infinite branches is like what was depicted in Figure 4(b) in Section 4, but we need to replace the configuration of 2×2 squares in that figure by using a configuration of $\infty \times \infty$ squares.

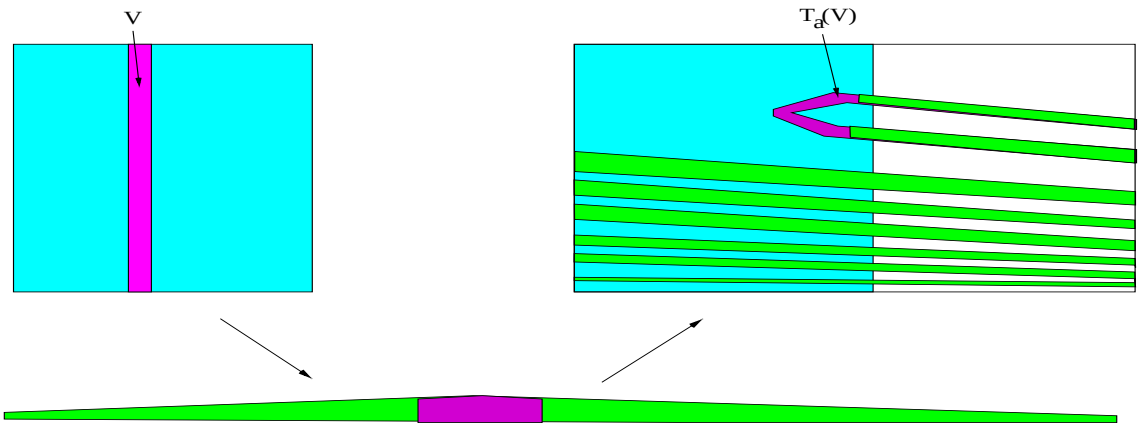

Figure 9. Infinitely Wrapped Horseshoe Map

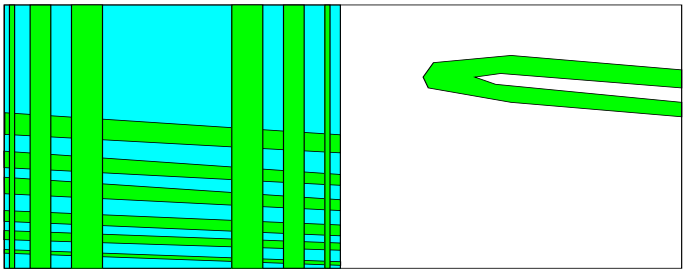

Figure 10. Horseshoe of infinitely many branches

Next we observe that there is an open set of a, for which the images of the folded part $\mathcal{T}_a(V)$ is placed back deep inside of D so that they are sufficiently close to V. For these parameters we have in V a strongly attractive periodic orbit for the corresponding maps. See Figure 11

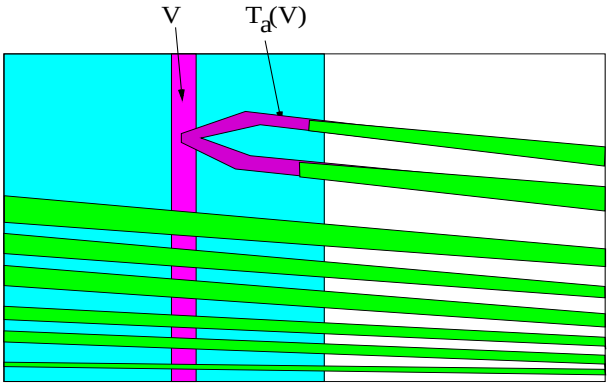

Figure 11. Strongly attractive stable periodic orbit

It takes some work to prove the existence of Newhouse tangency for $\mathcal{T}_a$, and this proof goes as follows (see [44] for a rigorous presentation). First, we observe that a horseshoe

of infinitely many branches exists for $\mathcal{T}_a$ for all a thanks to the *infinitely wrapped* nature of $T(D)$ in $\mathcal{A}$.[6] Second, taking a periodic orbit in this horseshoe, we can prove that the unstable manifold is a roughly horizontal curve in D, which we denote as ℓ_h. We can also prove that the stable manifold is a curve cutting vertically across $\mathcal{A}$ in D, which we denote as ℓ_v. The image of ℓ_h is a folded curve, which is dragged by our varying a to pass ℓ_v, inducing Newhouse tangency. See Figure 12.

Consequently, there is a positive measure set of a, so that $\mathcal{T}_a$ contain a strange attractor with an SRB measure of Benedick-Carleson and Young. It also follows from the Newhouse theory that there exists an open set of a so that $\mathcal{T}_a$ has stable periodic solution.

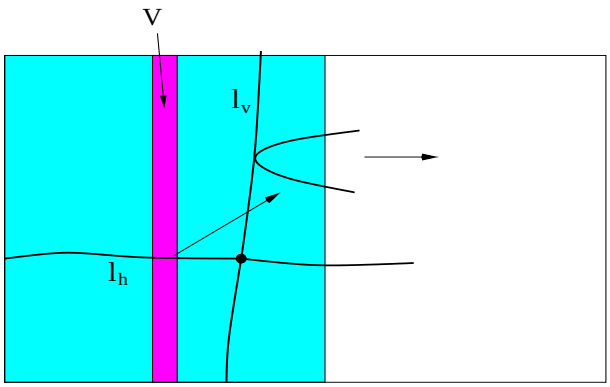

Figure 12. Transversal Homoclinic Tangency

(b) Organizations of invariant sets in parameter space We start with the obvious that the dynamics of $\mathcal{T}_a$ is 2π-periodic in a. This is to say that the invariant set defined by $\mathcal{T}_a$ is identical to that of $\mathcal{T}_{a+2\pi n}$ for all n. Second, the image of $\mathcal{T}_a(D)$ is dragged in $\mathcal{A}$ in the θ-direction as a varies, and the folded tip is moving at a speed of 1 with respect to a.

When the folded part of $\mathcal{T}_a(D)$ is dragged across the vertical boundaries of D, Newhouse tangency would happen in a way, the details of which are incomprehensibly complicated. Every saddle periodic orbit in that horseshoe of infinitely many branches is with a roughly horizontal unstable manifold and a rough vertical stable manifold. The unstable manifold would be mapped back as a folded curve, and as a varies, the folded tip would pass the stable manifold of all other saddles accumulating towards the vertical boundaries of D, inducing Newhouse Sinks and SRB measures of Benedicks-Carleson and Young. This infinitely refined structure of tangency remains a mystery to be unraveled.

(c) From the simulation standing of point As far as numerical plots are concerned, all the fine details of the impossibly complicated mingling of sinks and SRB measures would be erased by numerical error. We would be left with a dynamical structure of finite precision, in which three dynamical scenarios would likely to show up. They are: *(a) nothing at all; (b) stable periodic orbit; and (c) SRB measure of Benedicks-Carleson and Young.* We note that (a) happens when the folded part of $\mathcal{T}_a(D)$ is mapped out of D. In this case horseshoes do not show up in numerical plots: almost all orbits initiated in D would eventually be plotted out of D. The occurrence of (c) is due to the fact that the Lebesgue measure of the parameter set for chaotic Hénon maps are positive.

[6]We note that the presence of this horseshoe of infinitely many branches for all a makes $\mathcal{T}_a$ very different from the *partial horseshoe* characterized by putting the folded part of a Smale horseshoe back inside of its defining domain. For $\mathcal{T}_a$, there is one horseshoe for all a that is never only partially defined.

9. Dynamics of Homoclinic Tangles of Equation (3.2)

In this section we study the differential equation (3.2) assuming $x \in \mathbb{R}^2$. We first introduce an angular variable θ to rewrite it as

$$\frac{dx}{dt} = f(x) + \varepsilon g(x, \omega\theta), \qquad \frac{d\theta}{dt} = \omega^{-1} \tag{9.1}$$

where $\omega = 2\pi T^{-1}$ is the forcing frequency. The variables (x, θ) is in the *extended phase space* $\mathbb{R}^2 \times \mathbb{S}$. We assume $x = 0$ is a saddle fixed point of the unperturbed equation and it has a homoclinic solution.

In our study, we do *not* use the time-T map. In its stead we use the *separatrix map* introduced by Shilnikov ([38]). To construct the separatrix map, we start with a short segment intersecting the homoclinic solution in the space of x, which we denote as I. We extend I in the direction of θ to form an annulus $\mathcal{A} = \mathbb{S} \times I$ in the extended phase space. The separatrix map is the return map defined by the solutions of (9.1) from $\mathcal{A}$ back to $\mathcal{A}$. See Figure 13.

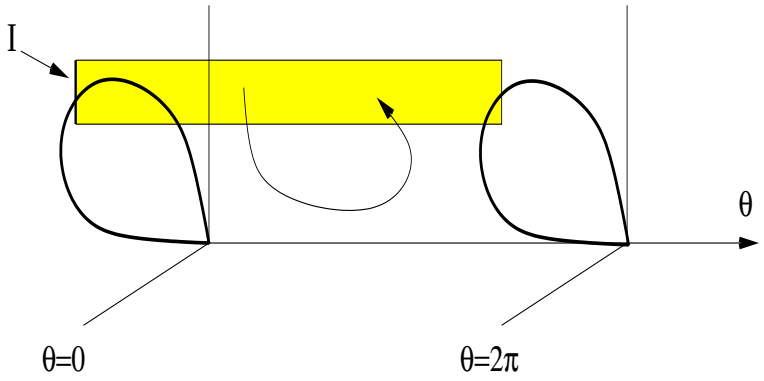

Figure 13. The Separatrix Map

The separatrix map, though not used as extensively as the time-T map in the study of differential equations, has been nevertheless employed as a technical alternative by many. It was the main technical tool in the construction of Shilnikov attractors ([39], [2], [10]). It has also been used as an alternative venues to study the Arnold diffusion in Hamiltonian equation ([29]).

Let $x = 0$ be a saddle fixed point of the unperturbed equation in x-space, β be the unstable eigenvalue, and $-\alpha$ be the stable eigenvalue of $x = 0$. We assume $x = 0$ is a *dissipative* saddle. This is to say that we assume

$$\alpha > \beta > 0. \tag{9.2}$$

We also assume that the unperturbed equation has a homoclinic solution $(x, y) = (a(t), b(t))$.

With these assumptions, Ali Oksasoglu and I computed the separatrix map $\mathcal{R} : \mathcal{A} \to \mathcal{A}$ in [44]. By a simple rescale, which resized I to $[-1, 1]$, we wrote the map $\mathcal{R}$ in terms of $(\theta, y) \in \mathbb{S} \times [-1, 1]$. We attained a formula for $\mathcal{R}$ for equation (9.1).

A major part of the derivation in [44] is to identify terms that do not alter the overall dynamics of $\mathcal{R}$. We caution that these term are not necessarily the usual error terms. Take the infinitely wrapped horseshoe map in the previous section as an example. We can add a large constant to the formula for θ_1 without effecting the overall dynamics of these maps.

With such terms removed, what remained for $\mathcal{R}$ is in the form of

$$\begin{aligned} \theta_1 =& \frac{\omega}{\beta}\ln\varepsilon^{-1} + \theta + \frac{\omega}{\beta}\ln(k_0 y + W(\theta)) \\ y_1 =& \varepsilon^{\frac{\alpha}{\beta}-1}(k_0 y + W(\theta))^{\frac{\alpha}{\beta}}. \end{aligned} \tag{9.3}$$

where k_0 is such that $\varepsilon << k_0 << 1$, and

$$W(\theta) = \int_{-\infty}^{+\infty} b(t)P(t+\theta, a(t), b(t))dt$$

is the classical Melnikov function.[7] In what follows we assume

(A1) *All zeros of $W(\theta)$ are non-tangential, and*
(A2) *all critical points of $W(\theta)$ are non-degenerate.*

We note that for a completely rigorous presentation we should use, in the place of (9.3), the rather detailed formula for $\mathcal{R}$ derived in [44], though at the end we would reach exactly the same conclusions. Here, we elect to use (9.3) to avoid a technically involved exposition. We refer the reader who is interested in a detailed rigorous mathematical encounter to [44].

The maps in (9.3) is a one parameter family, which we denote as $\mathcal{R}_\varepsilon$. We compare $\mathcal{R}_\varepsilon$ with the infinitely wrapped horseshoe maps $\mathcal{T}_a$ in (8.1). Looking at the θ_1 component, we see that the parameter a in $\mathcal{T}_a$ corresponds to

$$a = \frac{\omega}{\beta}\ln\varepsilon^{-1}$$

in $\mathcal{R}_\varepsilon$. However, $\mathcal{R}_\varepsilon$ is *not periodic* in a because ε is also involved in the y_1 component. Instead of a strict periodicity in parameter space, $\mathcal{R}_\varepsilon$ only admits an *asymptotic periodicity* with respect to a as $\varepsilon \to 0$. Conceptually, we can think of $\mathcal{R}_\varepsilon$ as a 2D extension of the 1D family

$$\theta_1 = a + \theta + \frac{\omega}{\beta}\ln(k_0 y + W(\theta))$$

where $a = \frac{\omega}{\beta}\ln\varepsilon^{-1} mod(2\pi)$. The periodicity of the dynamics of $\mathcal{R}_\varepsilon$ in parameter space is embedded asymptotically in this $1D$ family.

Second, the Melnikov function $W(\theta)$ takes the place of $\sin\theta$ in $\mathcal{T}_a$. This is to imply that the curves defined by

$$k_0 y + W(\theta) = 0$$

are the boundaries of the domain of $\mathcal{R}_\varepsilon$. All boundary curved are near vertical[8] and they would cut the annulus $\mathcal{A}$ into roughly rectangular regions. In general, the domain of $\mathcal{R}_\varepsilon$ is now allowed to have more than one rectangular region.

We further observe that the actions of $\mathcal{R}_\varepsilon$ on each of these rectangular regions are similar to the actions of $\mathcal{T}_a$ on D. It compresses it in the y-direction, and stretches it in the θ-direction to infinite length on both side. This image is then folded and place back,[9] with two infinitely long tails wrapping around $\mathcal{A}$ indefinitely. What is new here is that this image may be folded at more than one place depending on the shape of $W(\theta)$.

[7]Explicit formula for $W(\theta)$ was first acquired by Poincaré for a periodically perturbed pendulum to verify the existence of non-tangential intersection of stable and unstable manifold, then for many other equations in later studies (See [13]).

[8]This follows from assumption (A1) on $W(\theta)$ and $k_0 << 1$.

[9]These foldings are quadratic by assumption (A2) on $W(\theta)$. This is to allow Newhouse theory to apply.

In summary, homoclinic tangle of equation (9.1) is a one parameter family and ε is the parameter. On a parameter interval $[\varepsilon_1, \varepsilon_2]$ satisfying

$$\frac{\omega}{\beta}\ln\varepsilon_2 - \frac{\omega}{\beta}\ln\varepsilon_1 = 2\pi, \tag{9.4}$$

homoclinic tangles fit together in a predestined pattern that mimic what was outlined in the previous section for $\mathcal{T}_a$, $a \in [0, 2\pi]$, and this predestined pattern is repeated indefinitely in an asymptotic fashion as $\varepsilon \to 0$. Note that ω is the forcing frequency and β is the unstable eigenvalue of the fixed point $x = 0$.

Within one period of this repeating pattern, three dynamical scenarios are competing in parameter space. The first is the case in which the entire homoclinic tangle is a horseshoe of infinitely many branches, the second is that of an asymptotically stable periodic orbit; the third is that of an SRB measure of Benedicks-Carleson and Young. This dynamics pattern is exceedingly complicated around the values of ε at which the folded part of the images are dragged crossing the boundary curves of the domain of $\mathcal{R}_\varepsilon$ by our varying ε.

An Overview: Conceptually, we can regard the homoclinic tangles of second order equation (3.2) as a staged show that is casted around *one* horseshoe of infinitely many branches. Let D be a rectangular region on which the separatrix map $\mathcal{R}_\varepsilon$ is defined. The stage where this show is enacted is D. When the folded part of the image $\mathcal{R}_\varepsilon(D)$ is casted out of D in $\mathcal{A}$, the stage is darkened so this horseshoe is hidden from us in the sense that it is not observable in numerical simulations. When the folded part is dragged passing through D, the elements of this horseshoe are lighted up, **not all at once, but one by one**, through the light shed by Newhouse tangency.

The same staged show is enacted in infinite repetition as $\varepsilon \to 0$.

10. Result of Numerical Simulation

In this section we present a simulation result to confirm what was acclaimed at the end of the last section. We start with a second order equation

$$\frac{d^2x}{dt^2} + (\lambda - \gamma x^2)\frac{dx}{dt} - x + x^2 = 0 \tag{10.1}$$

where $\lambda, \gamma > 0$ are parameters. Let $y = dx/dt$. The point $(x, y) = (0, 0)$ is a dissipative saddle.

The first step of this simulation is to fix $\lambda = 0.5$ to find a value of γ for which $(x, y) = (0, 0)$ admits a homoclinic solution. This value is attained numerically as $\gamma = 0.577028548901$. We add a time-periodic term to equation (10.1) to obtain

$$\frac{d^2x}{dt^2} + (\lambda - \gamma x^2)\frac{dx}{dt} - x + x^2 = \varepsilon\sin 2\pi t. \tag{10.2}$$

The theory presented in the last section acclaims that, for equation (10.2), there is an arrangement of homoclinic tangles, relatively simple around certain values of ε (when the folded part of the image is out of the domain of the separatrix map), but exceedingly complicated around others (associated to Newhouse tangency). As $\varepsilon \to 0$, this arrangement is indefinitely repeated in parameter space ε. The infinitely refined details of this arrangement, on the other hand, would be erased by numerical error in simulation. Consequently, numerical simulation would produce a finite pattern in parameter space, in which three dynamic scenarios would show up in alternation and they are (a) homoclinic tangle that is composed entirely of one horseshoe of infinitely many branches, (b) homoclinic tangles dominated by assymptotically stable periodic orbit, and (c) Homoclinic tangles with SRB measure of Benedicks-Carleson and Young. In what follows we name (a) as *transient tangle*

because almost all orbits would be mapped out. We name (b) as *tangle with sink*, and (c) as *tangle with SRB measure*.

In [45] we tabulated the occurrence of these tangles. The simulation result is presented in Table 1.

TABLE 1. Multiplicative periodicity on ε.

$\lambda = 0.5,\ \gamma = 0.577028548901,\ \beta = 0.78077641,$ Predicted Multiplicative Period= 2.1831			
ε	Dynamical Behavior	Actual Ratio	Frequency of Occurrence (%)
$1.577 \cdot 10^{-3}$	Transient tangle	–	94.23
$7.774 \cdot 10^{-4}$	Tangle with SRB measure	–	1.61
$7.637 \cdot 10^{-4}$	Tangle with sink	–	4.16
$7.284 \cdot 10^{-4}$	Transient tangle	2.1650	94.28
$3.574 \cdot 10^{-4}$	Tangle with SRB measure	2.1752	3.18
$3.449 \cdot 10^{-4}$	Tangle with sink	2.2143	2.54
$3.349 \cdot 10^{-4}$	Transient tangle	2.1750	94.54
$1.635 \cdot 10^{-4}$	Tangle with SRB measure	2.1859	1.49
$1.608 \cdot 10^{-4}$	Tangle with sink	2.2143	3.97
$1.536 \cdot 10^{-4}$	Transient tangle	2.1803	94.42
$7.505 \cdot 10^{-5}$	Tangle with SRB measure	2.1785	2.37
$7.308 \cdot 10^{-5}$	Tangle with sink	2.2003	3.21
$7.041 \cdot 10^{-5}$	Transient tangle	2.1815	95.00
$3.415 \cdot 10^{-5}$	Tangle with SRB measure	2.1977	1.91
$3.342 \cdot 10^{-5}$	Tangle with sink	2.1867	3.09
$3.224 \cdot 10^{-5}$	Transient tangle	2.1839	94.29
$1.574 \cdot 10^{-5}$	Tangle with SRB measure	2.1696	3.17
$1.504 \cdot 10^{-5}$	Tangle with sink	2.2221	2.54
$1.474 \cdot 10^{-5}$	Transient tangle	2.1872	94.53
$7.190 \cdot 10^{-6}$	Tangle with SRB measure	2.1892	4.00
$6.931 \cdot 10^{-6}$	Tangle with sink	2.1700	1.71

The proper way to read the first two columns of this table is as follows: We start with $\varepsilon = 1.577 \cdot 10^{-3}$. For ε in between $1.577 \cdot 10^{-3}$ and $7.774 \cdot 10^{-4}$, simulation produces transient tangle. At $\varepsilon = 7.774 \cdot 10^{-4}$, tangle with SRB measure occurs in simulation. Then for ε in between $7.774 \cdot 10^{-4}$ and $7.637 \cdot 10^{-4}$, simulation produces tangle with SRB measure, but tangle with sink occurs at $\varepsilon = 7.637 \cdot 10^{-4}$, and so on.

There is clearly a repeated pattern as shown in Table 1. This pattern is anticipated in theory to be 2π-periodic with respect to $a = 2\pi\beta^{-1} \ln \varepsilon$ where β is the unstable eigenvalue of $(x, y) = (0, 0)$. This periodicity in a, reflected in ε, is *multiplicative*: this is to say letting ε_1 and ε_2 be the end points of an ε-interval such that

$$2\pi\beta^{-1} \ln \varepsilon_2 - 2\pi\beta^{-1} \ln \varepsilon_1 = 2\pi,$$

we have

$$\varepsilon_2 = e^{\beta} \varepsilon_1.$$

For equation (10.2) with $\lambda = 0.5,\ \gamma = 0.577028548901$, we have $\beta = 0.78077641$. The number $e^{\beta} = 2.1831$ is the theoretic prediction of the multiplicative period in ε-space.

The third column of Table 1 is the ratio of the ε value three lines above to the current ε value. To check the predicted multiplicative periodicity in parameter space, one compares these values to the predicted multiplicative period 2.1831. The last column of this table is self-explanatory. The low percentage for SRB measures partially explains why, in many numerical simulations of the past, one has to try hard in searching for such chaotic tangles.

In conclusion, results of numerical simulation clearly match the prediction of the theory presented in the last section. We refer the reader to [45] for a technically detailed presentation of this numerical simulation.

Acknowledgment: I would like to first thank my friends, Kening Lu and Zhihong Xia, for their long lasting friendship and support. I am also deeply in debt to my Ph.D. advisor Ken Meyer, my postdoctor mentor and long time collaborator Lai-Sang Young, and Don Saari, for their generous support over the years. Just want to take this opportunity to say that I am very, very grateful.

References

[1] V.M. Alekseev, *Quasiradom Dynamical Systems I, II, III*, Math. USSR Sbornik **5** (1968) 73-128, **6** (1968), 506-560, **7** (1969), 1-43.
[2] V.S. Afraimovich and L.P. Shil'nikov, *The ring principle in problems of interaction between two self-oscillating systems*, PMM Vol **41**(4), (1977), 618-627.
[3] D.V. Anosov, *Geodesic flows on compact manifolds of negative curvature*, Proc. Steklov Inst. Math., **90** (1967) 1-209.
[4] M. Benedicks and L. Carleson, *The dynamics of the Hénon map*, Ann. Math. **133** (1991), 73-169.
[5] M. Benedicks and M. Viana, *Solution of the basin problem for Hénon attractors*, Invent. Math. **143** (2001), 375-434.
[6] M. Benedicks and L.-S. Young, *Sinai-Ruelle-Bowen measures for certain Hénon maps*, Invent. Math. **112** (1993). 541-576.
[7] G.D. Birkhoff, *Nouvelles Recherches sur les systemes dynamiques* Mem. Pont. Acad.Sci. Novi Lyncaei, **1**, 85-216 (1935), in particular, Chapter IV.
[8] R. Bowen, *Periodic points and measures for Axiom A diffeomorphisms*, TAMS (1971), 377-397.
[9] K.L. Cartwright and J.E. Littlewood, *On non-linear differential equations of the second order, I: The equation* $\ddot{y} + k(1-y^2)\dot{y} + y = b\lambda k \cos(\lambda t + a), k$ *large*, J. London. Math. Soc. **20**, (1945), 180-189.
[10] B. Deng, *On Shilnikovs homoclinic saddle-focus theorem*, JDE 102 (1993) 305329.
[11] G. Duffing, *Erzwungene Schwingungen bei Veranderlicher Eigenfrequenz*, F. Wieweg u. Sohn: Braunschweig. (1918).
[12] M.J. Feigenbaum, *Quantitative universality for a class of non-linear transformations*, J. stat. Phys., **19** (1978) 25-52.
[13] J. Guckenheimer and P. Holmes, *nonlinear osscilations, dynamical systems and birfurcation of vector fields*, Springer-Verlag, Appl. Math. Sciences **42** (1983).
[14] D. Florin and P. Holmes, *Celestial encounters: the origins of chaos and stability*, Princeton University Press, Princeton, 1999.
[15] M. Hénon, *A two-dimensional mapping with a strange attractor*, Comm. Math. Phys. **50** (1976), 69-77.
[16] G. W. Hill *Works*, **1** (1878)
[17] N. Levinson, *A Second-order differential equaton with singular solutions*, Ann. Math. **50** (1949), 127-153.
[18] T.Y. Li and J.A. York, *Periodic three implies chaos*, Amer. Math. Monthly, **82** (1975) 985-992.
[19] K. Lin and L.-S. Young, *Shear-induced chaos*, Nonlinearity **21** (2008) 899-922.
[20] E. N. Lorenz, *Deterministic non-periodic flow*, J.Amer. Sci., **20** (1963), 130-141.
[21] C.K. McCord, K.R. Meyer and Q.D. Wang *The integral manifolds of the three body problem*, AMS Memoirs **132** (1998).
[22] R. McGehee, *Triple collision in collinear three-body problem.* Inventione Mathematicae, **27** (1974), 191-227.
[23] V.K. Melnikov, *On the stability of the center for time periodic perturbations*, Trans. Moscow Math. Soc., **12** (1963), 1-57.
[24] J. Milnor, *Morse Theory*, Princeton University Press, (1963).
[25] L. Mora and M. Viana, *Abundance of strange attractors*, Acta. Math. **171** (1993), 1-71.

[26] J.K. Moser, *Stable and random motions in dynsmical systems (with special emphasis on celestial mechanics)*, Princeton University Press, Princeton, NJ, (1973).

[27] S. E. Newhouse, *Diffeomorphisms with infinitely many sinks*, Topology, **13** (1974), 9-18.

[28] J. Palis and F. Takens, *Hyperbolicity & sensitive chaotic dynamics at homoclinic bifurcations*, Cambridge studies in advanced mathematics, **35** Cambridge University Press, Cambridge, (1993)

[29] G.N. Piftankin, D.V. Treschev, *Separatrix maps in Hamiltonian systems*, Russian Math. Surveys 62 (2) (2007) 219322.

[30] H. Poincaré, *Mémoire sur les courbes définies par une équation différetielle*, Journal de Mathematiques, **7** (1881), 375-422, and **8** (1882),251-296.

[31] H. Poincaré, *Sur le probléme des trios corps et les équations de la dynamique*, Acta Mathematica, **13** (1890), 1-270.

[32] H. Poincaré, *Les Méthodes Nouvelles de la Mécanique Céleste*, 3 Vols. Gauthier-Villars: Paris (1899)

[33] D. Ruelle, *Ergodic theory of differentiable dynamical systems*, Publ. Math., Inst. Hautes Étud. Sci. **50** (1979), 27-58.

[34] Y. G. Sinai, *Gibbs measure in ergodic theory*, Russian Math. Surveys **27** (1972), 21-69.

[35] C. L. Siegel and J. K. Moser *Lecture on celestial mechanics*, Springer-Verlag, 1971.

[36] S. Smale, *Generalized Poincaré's conjecture in dimensions greater than four*, Annals of Mathematics. **74**(2), (1961) 391406.

[37] S. Smale, *Diffeomorphisms with many periodic points*, Differential and Combinatorial Topology (A Symposium in Honor of Marston Morse), Princeton University Press, (1965), 63-80.

[38] L.P. Shilnikov, *A case of the existence of a countable number of periodic motion*, Sov. Math. Dokl. 6 (1965) 163166.

[39] L. P. Shilnikov, *On a Poincaré-Birkhoff Problem*, Math USSR-sb. 3 (1967), 353-371.

[40] K. Sitnikov, *existence of oscillating motions for the three-body problem*, Dokl. Akad. Nauk, USSR, **133**(2), (1960), 303-306.

[41] K. Sundman. *Recherches sur le problème des trois corps*, Acta, Mathematica, 36 (1912) 105-179.

[42] van der Pol B. and van der Mark J., *Frequency demultiplication*, Nature **120** (1927), 363-364.

[43] Q.D. Wang. *The Global Solution of N-body Problem*, Celest. Mech. 50, (1991) 73-88.

[44] Q.D. Wang and A. Oksasoglu, *Dynamics of Homoclinic Tangles in Periodically Perturbed Second Order Equations*, JDE 250(2011) 710-751.

[45] Q.D. Wang and A. Oksasoglu, *Periodic Occurrence of Dynamical Behavior of Homoclinic Tangles*, Physica D: Nonlinear Phenomena 239(7) (2010), 387-395.

[46] Q.D. Wang and L.-S. Young, *Strange attractors with one direction of instability*, Commun. Math. Phys., **218** (2001), 1-97.

[47] Q.D. Wang and L.-S. Young *Toward a Theory of Rank One Attractors*, Annals. Math. 167 (2008), 349-480.

[48] Q.D. Wang and L.-S. Young *Dynamical Profile of a Class of Rank One Attractors*, Ergodic Theory and Dynamical Systems 33(4) (2013) 1221-1264.

[49] Q.D. Wang and L.-S. Young *Strange attractors in periodically-kicked limit cycles and Hopf bifurcations*, Commun. Math. Phys. **24** (2003), 509-529.

[50] A. Wintner *The Analytic Foundations of Celestial Mechanics*, Princeton University Press, (1941).

[51] Z.H. Xia *The existence of noncollision singularities in the N-body problem*, Annals of Mathematics, **135** (1992), 411-468.